

# Tip-Scan High-Speed Atomic Force Microscopy in Organic Solvent: A Versatile Tool for Visualizing Dynamic Behaviors of Soft-Materials

Honami Matsui, Christian Ganser, Kenta Tamaki, Qiming Liu, Feng-Yueh Chan, Takayuki Uchihashi, Prabhat Verma, Yoshimitsu Sagara, Shiki Yagai, and Takayuki Umakoshi\*



Cite This: *Langmuir* 2026, 42, 448–454



Read Online

ACCESS |



Metrics & More

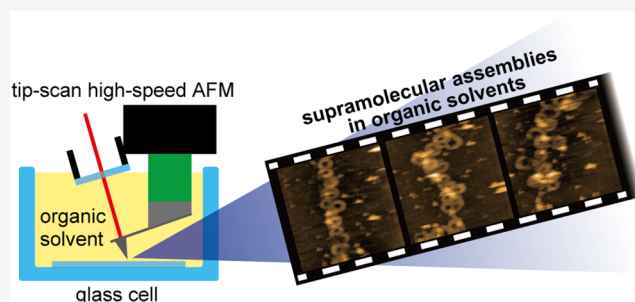


Article Recommendations



Supporting Information

**ABSTRACT:** High-speed atomic force microscopy (HS-AFM) is a powerful tool for video recording the nanoscale dynamics of samples. Its applications have recently expanded to various fields from biology to chemistry, including supramolecular chemistry and polymer science. Furthermore, the development of a stand-alone tip-scan HS-AFM has offered greater flexibility in installation. As it can be mounted on an optical microscope for integration with optical techniques, it holds great promise for supramolecular chemistry and polymer science. However, tip-scan HS-AFM observations in organic solvents have been challenging due to difficulties in holding them with low surface tension. In this study, we achieved tip-scan HS-AFM observations in organic solvents by developing a glass cell. The cell was carefully designed to be compatible with tip-scan HS-AFM operation in organic solvents. Using the cell, we successfully demonstrated tip-scan HS-AFM observations of supramolecular assemblies in various organic systems. In addition, the large and stable design of the cell allowed for a wider variety of organic solvents than the small wells used in conventional HS-AFM. Tip-scan HS-AFM compatible with organic solvents will contribute to investigating the complex dynamics of supramolecular assemblies and polymers in their native organic environments.



## INTRODUCTION

High-speed atomic force microscopy (HS-AFM) is a powerful technique for visualizing the nanoscale dynamics of biological samples under physiological conditions with high spatiotemporal resolution.<sup>1</sup> It has significantly advanced life sciences through the video recording of dynamic conformational changes of proteins at the single molecular level,<sup>2–6</sup> such as walking myosin V,<sup>7</sup> rotation of rotorless F<sub>1</sub>-ATPase,<sup>8</sup> and cleavage of IgG antibody.<sup>9</sup> Moreover, the application of this excellent imaging capability has recently been expanded to various disciplines. One of the critical applications is in the chemical field, particularly in supramolecular chemistry and polymer science.<sup>10–19</sup> HS-AFM has revealed various dynamics of supramolecular assemblies and polymers, such as the growth and self-healing of supramolecular fibers,<sup>11</sup> polymerization/depolymerization of supramolecular toroids,<sup>12</sup> and elongation of supramolecular gels.<sup>13</sup> These dynamic behaviors have been successfully observed in organic solvents, such as methylcyclohexane (MCH), dodecane, and dimethyl sulfoxide. While HS-AFM has already been an essential tool in biological research, it holds great promise for investigating complex molecular dynamics in chemistry.

Moreover, the recent development of tip-scan stand-alone HS-AFM has further enhanced its capability and extended its applications.<sup>20,21</sup> The tip-scan HS-AFM adopts the tip-scan

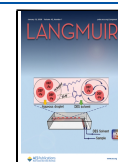
configuration, whereas conventional HS-AFM scans the sample stage. One of the most crucial advantages of tip-scan HS-AFM is flexibility in the installation location. The stand-alone HS-AFM system can be mounted on, for example, an inverted optical microscope, as shown in Figure 1a, which enables the integration of HS-AFM with various optical techniques to drastically improve its analytical ability.<sup>22</sup> Therefore, tip-scan HS-AFM holds great potential for observing various samples or phenomena that cannot be observed with the conventional type. For example, it allows for the local excitation of samples by a focused laser and simultaneous observation with HS-AFM. Also, it is possible to locally detect optical signals from samples, such as Raman scattering and photoluminescence. Indeed, we recently reported an HS-AFM movie of dynamic motions of azo-polymer thin films induced by local laser excitation.<sup>23</sup> In addition, although normal HS-AFM requires small samples that can be loaded on a small sample stage (diameter: 1–2 mm) of the high-speed stage scanner, tip-scan

**Received:** August 24, 2025

**Revised:** November 24, 2025

**Accepted:** December 9, 2025

**Published:** December 22, 2025



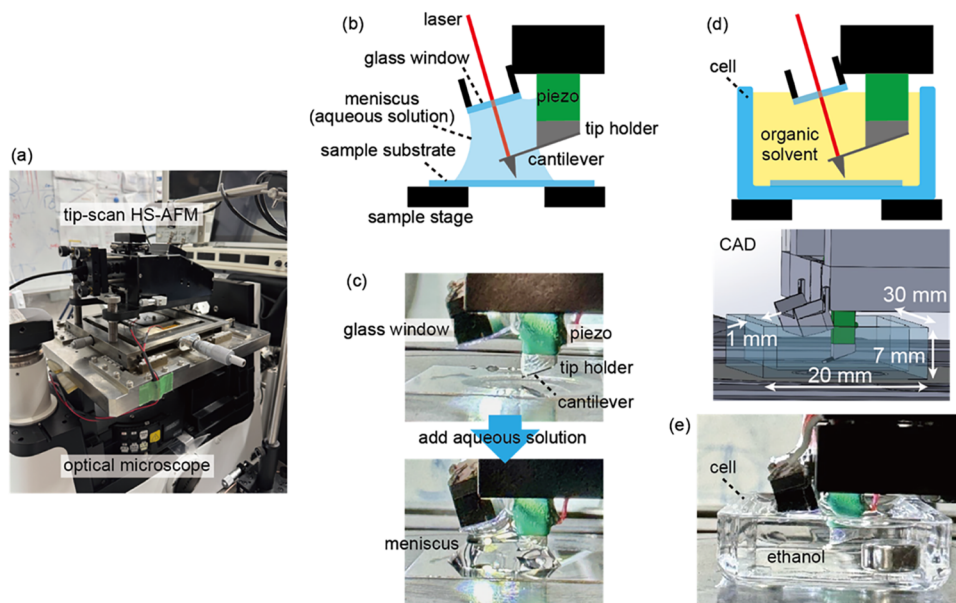


**Figure 1.** (a) Overview of the tip-scan HS-AFM. (b) Schematic configuration of tip-scan HS-AFM around the tip scanner. (c) Photographs around the tip scanner with and without aqueous solution. (d) Schematic configuration and three-dimensional (3D) CAD image of the cell with the tip scanner. (e) Photograph of the cell filled with ethanol and the tip immersed in it.

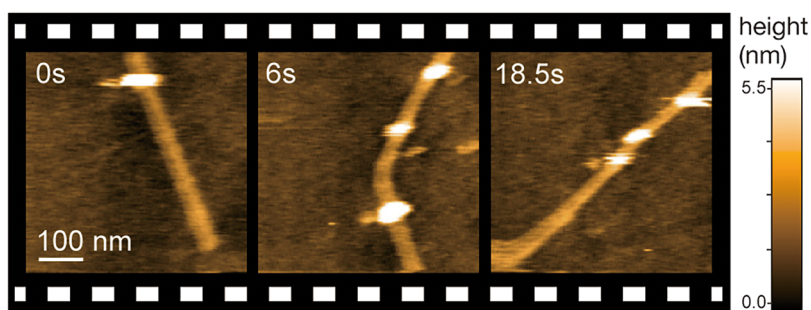


**Figure 2.** Clipped HS-AFM images of CNTs observed at 4 fps in ethanol.

HS-AFM possesses much fewer limitations to samples. A normal glass substrate or even a large device is available for tip-scan HS-AFM to observe their top surfaces.<sup>24,25</sup>

The superior versatility and analytical capability of tip-scan HS-AFM are highly desirable for studying supramolecular assemblies and polymers; however, its application to these samples remains challenging. Figure 1b shows a schematic around the tip scanner in the tip-scan HS-AFM. In the case of the tip-scan HS-AFM observation in an aqueous solution, we added a solution that forms a meniscus between the sample substrate and glass window, as shown in Figure 1c. This ensures proper optical access of the tip-scan HS-AFM laser through the glass window for the optical level system. However, the dynamic processes of supramolecular polymers often occur in organic solvents, where a meniscus cannot be formed due to its low surface tension. This limitation has prevented us from observing samples in organic solvents. In contrast, owing to a small well that holds the solvents, conventional HS-AFM has been used in organic solvents. By making the well compatible with tip-scan HS-AFM, direct observation of chemical reactions in organic solvents becomes possible, which further expands its applicability and contributes to chemistry, especially to supramolecular chemistry and polymer science.

In this study, we achieved tip-scan HS-AFM observations in organic solvents by designing and developing a cell for holding an organic solution. The cell structure was optimally designed to secure optical access for the HS-AFM laser but not to spatially interfere with the tip-scan HS-AFM components. We successfully demonstrated tip-scan HS-AFM observations in ethanol. We further applied it for the observation of different types of supramolecular assemblies in different organic media. Importantly, it was found that our cell is compatible with more various types of organic solvents compared with the small well used in conventional HS-AFM. This technical development is crucial for future applications of tip-scan HS-AFM in organic chemistry and related fields.

## EXPERIMENTAL SECTION

Figure 1d shows a schematic of the cell, including a side view and its 3D design, illustrating its dimensions of 7 mm in height, 30 mm in width, and 20 mm in length. The detail of the cell structure was described in Section 1.1 of the Supporting Information. The height of the cell is a critical parameter that requires optimization. If the value is too high, it spatially interferes with the tip scanner and disturbs the measurement. If it is too low, then the solution poured into the cell cannot touch the glass window for proper optical access. We chose a height of 7 mm, as it satisfies both conditions. We chose glass as the cell material, with a thickness of 1 mm, owing to its chemical stability

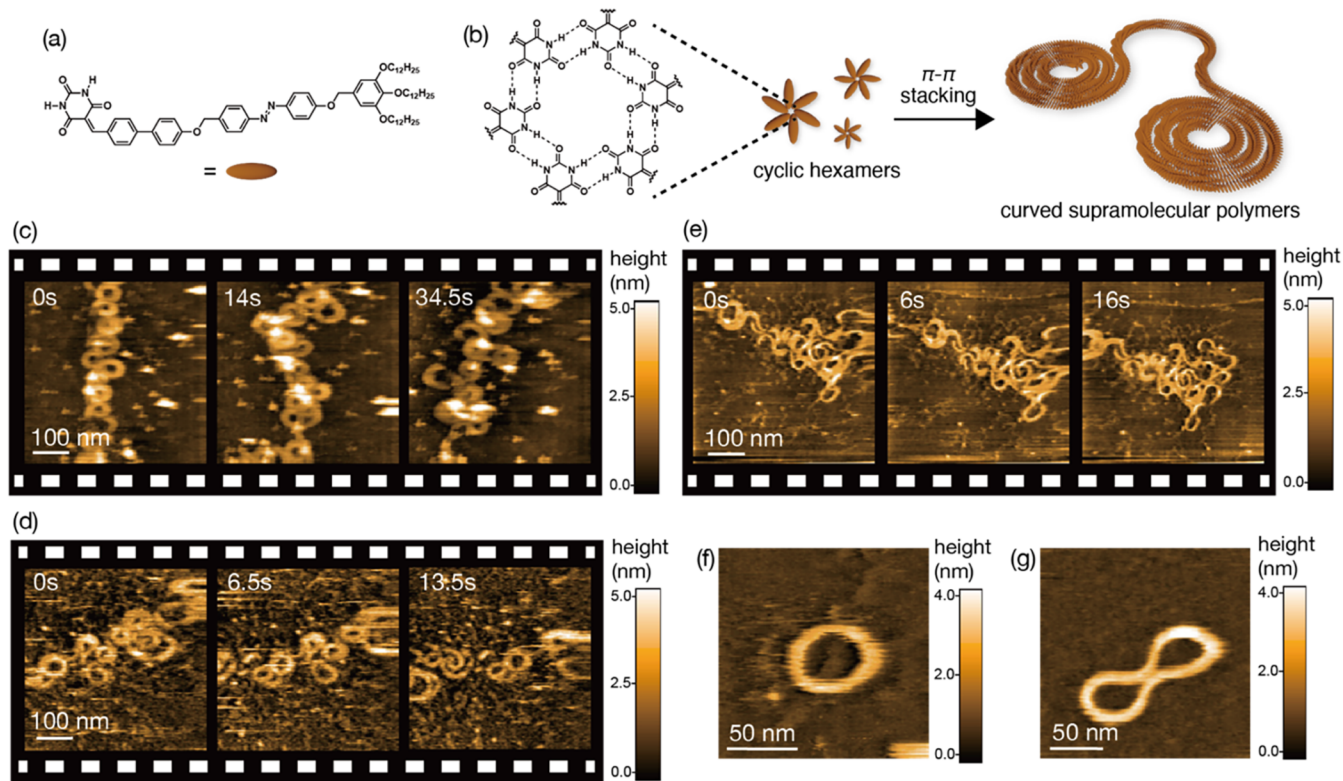


**Figure 3.** (a) Molecular structure of monomer 1. (b) Aggregation scheme of curved supramolecular polymers. (c–e) Clipped HS-AFM images of curved supramolecular polymers in (c) *n*-octane, (d) *n*-hexane, and (e) 2,2,4-trimethylpentane. (f) HS-AFM image of the ring-shaped supramolecular polymer in *n*-hexane. (g) HS-AFM image of the supramolecular polymer in an infinity-symbol-like shape observed in *n*-octane.

against organic solutions and optical transparency. Figure 1e shows a photograph of a glass cell (manufactured by ASONE) installed in a tip-scan HS-AFM system. The glass cell was filled with 2.5 mL of ethanol, and an end portion of the Z piezo scanner, which holds the cantilever, was immersed in the solution. We confirmed that the cell stably held the organic solvent. Furthermore, the upper part of the scanner did not touch the rim of the cell, and therefore did not interfere with the HS-AFM operation. In addition, the glass window, positioned on the laser optical path, was sufficiently immersed in ethanol for proper optical access.

## RESULTS AND DISCUSSION

To assess the compatibility of the cell with tip-scan HS-AFM observations in organic solvents, we observed carbon nanotubes (CNTs) as samples in ethanol. CNTs (IsoNanotubes-S, NanoIntegris) dispersed in 2-propanol were spin-coated on a cleaned glass substrate. This substrate was then placed in the glass cell and observed by tip-scan HS-AFM in ethanol. As shown in Figure 2 and Supporting Movie S1, we successfully achieved HS-AFM observation in ethanol at 4 frames per second (fps). The CNTs were clearly observed without any obvious issues. There were no noticeable differences in the operation of HS-AFM compared to that in an aqueous solution. Furthermore, the resonance frequency of the cantilevers in ethanol was found to be approximately 400 kHz, which is almost identical with that in water. The experimental details of HS-AFM measurements were described in Section 1.2 of the Supporting Information.

As we confirmed that cell-equipped tip-scan HS-AFM was available for synthetic samples in organic solvents, we expanded the observation target toward supramolecular polymers. Supramolecular polymers are promising polymeric

materials that are formed through weak intermolecular interactions between monomers.<sup>26–34</sup> Precisely designed and organized interactions allow supramolecular polymers to exhibit various interesting characteristics. Through meticulous molecular design and supramolecular polymerization protocols, we can create supramolecular polymers with a variety of interesting shapes, such as fibers,<sup>35</sup> rings,<sup>36</sup> helicoids,<sup>37</sup> and catenanes.<sup>38</sup> As they are assemblies of numerous monomers, they can be relatively easily observed through AFM, which also makes supramolecular polymers a great candidate that HS-AFM can effectively contribute to. Although the dynamic behavior of supramolecular polymers has been reported by several research groups, such studies remain relatively scarce.<sup>11–16</sup> In particular, there have been no reports on the observation of supramolecular polymers using tip-scan HS-AFM.

Here, we explored the applicability of tip-scan HS-AFM to curved supramolecular polymers formed by monomer 1 shown in Figure 3a.<sup>14</sup> Supramolecular polymers were prepared in MCH following a previously reported protocol.<sup>14</sup> The monomers first formed cyclic hexamers, which were subsequently piled up through  $\pi$ - $\pi$  stacking to form curved supramolecular polymers, as shown in Figure 3b. For the HS-AFM observation, the polymers were spin-coated onto a highly oriented pyrolytic graphite (HOPG) substrate. Subsequently, the substrate was placed in the cell and imaged in *n*-octane. As shown in Figure 3c and Supporting Movie S2, long and clearly curved supramolecular polymers were successfully visualized in the organic solvent. This demonstrates that tip-scan HS-AFM, when combined with the developed observation cell, enables high-resolution imaging of supramolecular structures even in

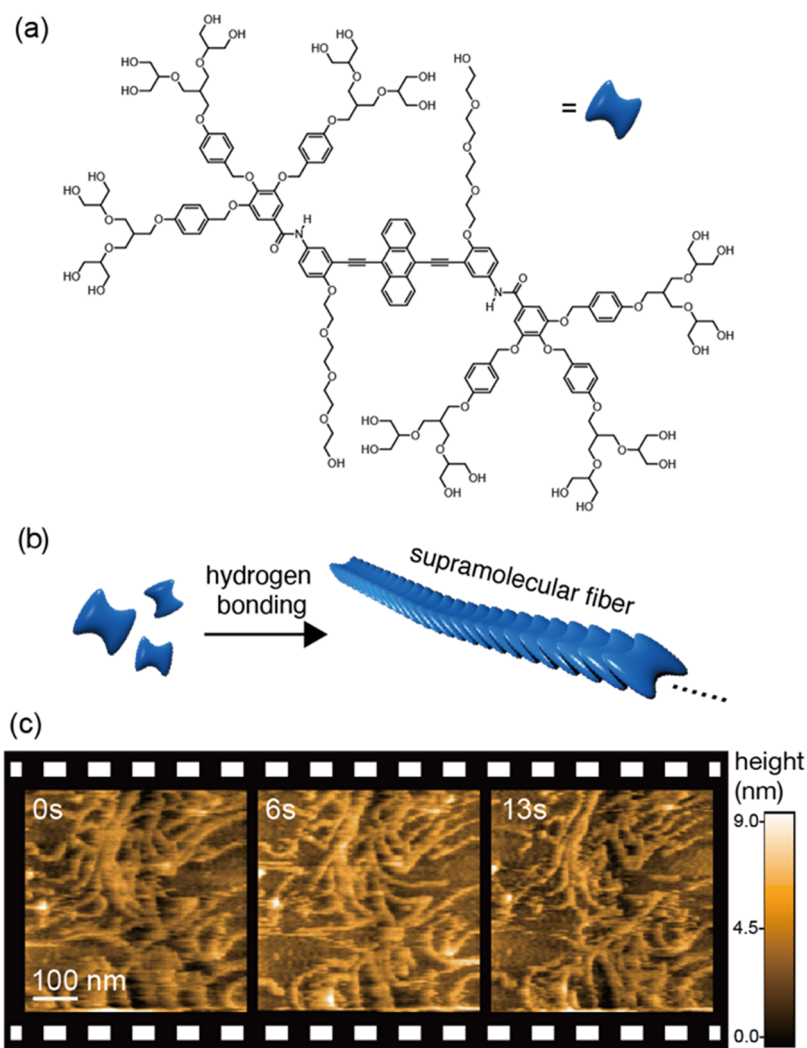


**Figure 4.** (a) Molecular structure of monomer 2. (b) Aggregation scheme of the supramolecular fiber. (c) Clipped HS-AFM images of supramolecular fibers observed in the methanol/water mixture (methanol/water = 2:8 v/v).

organic media—a significant step toward broadening its utility in soft matter and supramolecular polymer materials.<sup>14</sup>

We also tested other organic solvents such as *n*-hexane and 2,2,4-trimethylpentane for tip-scan HS-AFM observations. Curved supramolecular polymers were also observed in these organic solvents, as shown in Figure 3d,3e and in Supporting Movies S3 and S4. However, the substrate was not clean, and the HS-AFM images were not so clear in the case of *n*-hexane. This is probably because the monomers were attached to the substrate due to its relatively low solubility in *n*-hexane. Furthermore, we found that the supramolecular polymers were more densely attached to the substrate in 2,2,4-trimethylpentane, as we could easily find different supramolecular polymers (Supporting Movies S5 and S6). This phenomenon is likely attributable to the weaker interaction between 2,2,4-trimethylpentane and the supramolecular polymers surrounded by *n*-dodecyl chains, compared with *n*-octane and *n*-hexane. It is also worth noting that *n*-hexane and 2,2,4-trimethylpentane have been unsuitable for use in conventional HS-AFM. This unsuitability stems from the reliance of the conventional system on a small (volume:  $\sim 80 \mu\text{L}$ ) and slightly tilted (several degrees) well to hold the observation solvent. With low surface tension and volatile solvents such as *n*-hexane and 2,2,4-trimethylpentane, the liquid often fails to remain stably in the

well, making consistent and stable imaging difficult. In contrast, our custom cell used in tip-scan HS-AFM features a flat base and a much larger volume ( $\sim 2.5 \text{ mL}$ ), thereby allowing for the stable retention of a wider variety of organic solvents, including those previously incompatible. This enhanced compatibility represents a key advantage of our cell, especially given that supramolecular behavior is often highly dependent on the nature of the solvent environment.<sup>38–41</sup>

We found not only open-ended (randomly coiled) curved supramolecular polymers but also closed-ended circular species at different locations in *n*-hexane and *n*-octane (Figure 3f,3g, and Supporting Movies S7 and S8). Figure 3f shows a closed ring-shaped structure, whereas Figure 3g shows a longer closed fiber with an infinity-symbol-like shape. Here, we also confirmed that the supramolecular polymers could be observed at most at an imaging rate of 5 fps in an organic solvent, as shown in Supporting Movie S9.

To confirm that our apparatus combining tip-scan HS-AFM with the cell is reliable and versatile, we investigated another supramolecular polymer consisting of monomer 2 (Figure 4a).<sup>42</sup> Dumbbell-shaped monomer 2 contains hydrophobic 9,10-bis(phenylethynyl)anthracene as the fluorescence core. In this molecule, 2 hydrophilic dendrons having 12 hydroxy groups at the peripheral positions were introduced to the

fluorophore via amide groups that form intermolecular hydrogen bonds. Therefore, monomer **2** is amphiphilic. Amphiphiles are known to form supramolecular assemblies in aqueous solutions.<sup>42–47</sup> The detailed synthetic procedures, analysis of the molecular assemblies in the supramolecular fibers, and stimuli-responsive luminescence properties are described in a previous study.<sup>42</sup> Monomer **2** was first dissolved in methanol, and Milli-Q water was then added so that the methanol/water ratio was 2:8 v/v, resulting in the formation of supramolecular fibers through hydrogen bonding due to the amphiphilic nature, as illustrated in Figure 4b. We dropped and spin-coated the solution on a HOPG substrate and observed it in a mixture of methanol and water (ratio = 2:8 v/v). Even though the solvent mostly consists of water, 20% methanol is already a concentration high enough to lower the solvent's surface tension, preventing the formation of a stable meniscus. Therefore, the glass cell is critical, even with such a solvent mostly composed of water. Using the glass cell, as shown in Figure 4c and Supporting Movie S10, we clearly observed supramolecular fibers in the water/methanol mixture. This successful observation confirmed that the short supramolecular fibers were densely distributed on the substrate. We also found that the supramolecular fibers were largely fluctuating in this solution, which could be revealed owing to the high-speed observation of tip-scan HS-AFM. We confirmed that our cell-equipped tip-scan HS-AFM is applicable to different types of supramolecular assemblies.

## CONCLUSIONS

In this study, we successfully developed a novel glass cell for tip-scan HS-AFM, which enables stable imaging in organic solvent systems. We demonstrated the excellent applicability of this cell through the successful imaging of various supramolecular assemblies in diverse organic solvents, including ethanol, *n*-hexane, *n*-octane, and 2,2,4-trimethylpentane. A key finding was the enhanced compatibility of our large and stable cell with a wider variety of organic solvents compared to the small wells typically used in conventional HS-AFM, which are often limited by low surface tension and volatility. Any organic solvents, except those with extremely high solvency, can be applied to our glass cell. It should also be noted that the glass cell significantly enhanced solvent retention time owing to its larger solvent volume compared with the small well used in normal HS-AFM. For example, stable imaging in *n*-octane was possible for at least 30 min without refilling the solvent when using our glass cell, whereas solvent replenishment was required approximately every 5 min for normal HS-AFM measurements. This greatly improves practical usability.

While the present study focused solely on tip-scan HS-AFM observations in organic solvents, it is important to emphasize that a significant advantage of tip-scan HS-AFM is its inherent compatibility with various optical techniques. We expect that the developed cell, when combined with tip-scan HS-AFM, will contribute significantly to elucidating the complex dynamics of supramolecular assemblies and other systems by enabling integrated optical measurements in the future. Indeed, the supramolecular polymers investigated in this study exhibit characteristic optical properties, making them particularly promising targets for such combined investigations. One of the potential limitations in the present glass cell is that it requires the use of a low numerical aperture objective due to the 1 mm-thick glass at the bottom, which compromises both spatial resolution and detection sensitivity. We expect that this

issue can be addressed either by thinning the bottom glass or by creating an aperture to attach a thin coverslip underneath the cell. We believe that this advancement will broaden the applicability of tip-scan HS-AFM, allowing its application to a wider range of research fields, including supramolecular chemistry and polymer science.

## ASSOCIATED CONTENT

### Supporting Information

The Supporting Information is available free of charge at <https://pubs.acs.org/doi/10.1021/acs.langmuir.5c04454>.

Detailed structure of the glass cell, experimental conditions of tip-scan HS-AFM, and HS-AFM movies of CNTs and supramolecular assemblies (PDF)

HS-AFM movie of CNTs in ethanol, shown in Figure 2; the movie was captured in a 500 × 500 nm<sup>2</sup> range, 150 × 150 pixels, at 4 fps (MP4)

HS-AFM movie of curved supramolecular polymers in *n*-octane shown in Figure 3c, captured in a 500 × 500 nm<sup>2</sup> range, 150 × 150 pixels, at 2 fps (MP4)

HS-AFM movie of curved supramolecular polymers in *n*-hexane shown in Figure 3d, captured in a 500 × 500 nm<sup>2</sup> range, 150 × 150 pixels, at 2 fps (MP4)

HS-AFM movie of curved supramolecular polymers in 2,2,4-trimethylpentane shown in Figure 3e, captured in a 500 × 500 nm<sup>2</sup> range, 150 × 150 pixels, at 2 fps (MP4)

HS-AFM movie of curved supramolecular polymers in 2,2,4-trimethylpentane shown, captured in a 500 × 500 nm<sup>2</sup> range, 150 × 150 pixels, at 2 fps (MP4)

HS-AFM movie of curved supramolecular polymers in 2,2,4-trimethylpentane shown, captured in a 500 × 500 nm<sup>2</sup> range, 150 × 150 pixels, at 2 fps (MP4)

HS-AFM movie of a ring-shaped supramolecular polymer in *n*-hexane shown in Figure 3f, captured in a 150 × 150 nm<sup>2</sup> range, 150 × 150 pixels, at 2 fps (MP4)

HS-AFM movie of the supramolecular polymer in an infinity-symbol-like shape in *n*-octane shown in Figure 3g, captured in a 200 × 200 nm<sup>2</sup> range, 150 × 150 pixels, at 2 fps (MP4)

HS-AFM movie of the supramolecular polymer in an infinity-symbol-like shape in *n*-octane, captured in a 200 × 200 nm<sup>2</sup> range, 150 × 150 pixels, at 5 fps (MP4)

HS-AFM movie of supramolecular fibers in a mixture of methanol and water (methanol/water = 2:8 v/v) shown in Figure 4c, captured in a 500 × 500 nm<sup>2</sup> range, 150 × 150 pixels, at 2 fps (MP4)

## AUTHOR INFORMATION

### Corresponding Author

Takayuki Umakoshi – Department of Applied Physics, The University of Osaka, Suita, Osaka 565-0871, Japan; Institute for Advanced Co-Creation Studies, The University of Osaka, Suita, Osaka 565-0871, Japan; [orcid.org/0000-0002-0479-1124](https://orcid.org/0000-0002-0479-1124); Email: [umakoshi@ap.eng.osaka-u.ac.jp](mailto:umakoshi@ap.eng.osaka-u.ac.jp)

### Authors

Honami Matsui – Department of Applied Physics, The University of Osaka, Suita, Osaka 565-0871, Japan

Christian Ganser – Exploratory Research Center on Life and Living Systems, National Institutes of Natural Sciences, Okazaki, Aichi 444-8787, Japan; [orcid.org/0000-0002-5558-3026](https://orcid.org/0000-0002-5558-3026)

**Kenta Tamaki** – Department of Physics, Nagoya University, Nagoya, Aichi 464-8602, Japan; [orcid.org/0000-0002-2553-8179](https://orcid.org/0000-0002-2553-8179)

**Qiming Liu** – Department of Materials Science and Engineering, Institute of Science, Tokyo, Tokyo 152-8552, Japan

**Feng-Yueh Chan** – Department of Physics, Nagoya University, Nagoya, Aichi 464-8602, Japan

**Takayuki Uchihashi** – Exploratory Research Center on Life and Living Systems, National Institutes of Natural Sciences, Okazaki, Aichi 444-8787, Japan; Department of Physics, Nagoya University, Nagoya, Aichi 464-8602, Japan

**Prabhat Verma** – Department of Applied Physics, The University of Osaka, Suita, Osaka 565-0871, Japan; [orcid.org/0000-0002-7781-418X](https://orcid.org/0000-0002-7781-418X)

**Yoshimitsu Sagara** – Department of Materials Science and Engineering, Institute of Science, Tokyo, Tokyo 152-8552, Japan; Research Center for Autonomous Systems Materialogy (ASMat), Institute of Integrated Research, Institute of Science Tokyo, Yokohama, Kanagawa 226-8501, Japan; [orcid.org/0000-0003-2502-3041](https://orcid.org/0000-0003-2502-3041)

**Shiki Yagai** – Institute for Advanced Academic Research and Department of Applied Chemistry and Biotechnology, Chiba University, Chiba 263-8522, Japan; [orcid.org/0000-0002-4786-8603](https://orcid.org/0000-0002-4786-8603)

Complete contact information is available at:

<https://pubs.acs.org/10.1021/acs.langmuir.5c04454>

### Author Contributions

T. Umakoshi conceived and designed this project. H.M., C.G., K.T., and T. Umakoshi performed experiments. H.M. analyzed the results and wrote the manuscript. C.G., F.-Y.C., T. Uchihashi, and T. Umakoshi constructed the experimental setup and supported the operation. K.T., Q.L., Y.S., and S.Y. prepared the samples. All authors contributed to the discussion and finalization of the manuscript.

### Notes

The authors declare no competing financial interest.

### ACKNOWLEDGMENTS

This work was partially supported by JST FOREST (JPMJFR233Z), JSPS Grant-in-Aid for Scientific Research (KAKENHI) (Grant-in-Aid for Transformative Research Areas (A) “Materials science of meso-hierarchy” JP24H01717, JP23H04873, and JP23H04878, Grant-in-Aid for Scientific Research (B) JP24K01385, Grant-in-Aid for Transformative Research Areas (A) “Chiral materials science pioneered by the helicity of light” JP23H04590, Grant-in-Aid for Challenging Research (Exploratory) JP24K21718), and a research grant from the Takahashi Industrial and Economic Research Foundation. K.T. acknowledges the JSPS for a Research Fellowship for Young Scientists (JP22KJ0486).

### REFERENCES

- (1) Ando, T.; Kodera, N.; Takai, E.; Maruyama, D.; Saito, K.; Toda, A. A High-Speed Atomic Force Microscope for Studying Biological Macromolecules. *Proc. Natl. Acad. Sci. U.S.A.* **2001**, *98* (22), 12468–12472.
- (2) Shibata, M.; Yamashita, H.; Uchihashi, T.; Kandori, H.; Ando, T. High-Speed Atomic Force Microscopy Shows Dynamic Molecular Processes in Photoactivated Bacteriorhodopsin. *Nat. Nanotechnol.* **2010**, *5* (3), 208–212.

- (3) Kobayashi, M.; Sumitomo, K.; Torimitsu, K. Real-Time Imaging of DNA–Streptavidin Complex Formation in Solution Using a High-Speed Atomic Force Microscope. *Ultramicroscopy* **2007**, *107* (2–3), 184–190.

- (4) Casuso, I.; Khao, J.; Chami, M.; Paul-Gilloteaux, P.; Husain, M.; Duneau, J.-P.; Stahlberg, H.; Sturgis, J. N.; Scheuring, S. Characterization of the Motion of Membrane Proteins Using High-Speed Atomic Force Microscopy. *Nat. Nanotechnol.* **2012**, *7* (8), 525–529.

- (5) Shibata, M.; Nishimasu, H.; Kodera, N.; Hirano, S.; Ando, T.; Uchihashi, T.; Nureki, O. Real-Space and Real-Time Dynamics of CRISPR-Cas9 Visualized by High-Speed Atomic Force Microscopy. *Nat. Commun.* **2017**, *8* (1), No. 1430.

- (6) Kanaoka, Y.; Mori, T.; Nagaike, W.; Itaya, S.; Nonaka, Y.; Kohga, H.; Haruyama, T.; Sugano, Y.; Miyazaki, R.; Ichikawa, M.; Uchihashi, T.; Tsukazaki, T. AFM Observation of Protein Translocation Mediated by One Unit of SecYEG-SecA Complex. *Nat. Commun.* **2025**, *16* (1), No. 225.

- (7) Kodera, N.; Yamamoto, D.; Ishikawa, R.; Ando, T. Video Imaging of Walking Myosin v by High-Speed Atomic Force Microscopy. *Nature* **2010**, *468* (7320), 72–76.

- (8) Uchihashi, T.; Iino, R.; Ando, T.; Noji, H. High-Speed Atomic Force Microscopy Reveals Rotary Catalysis of Rotorless F1-ATPase. *Science* **2011**, *333* (6043), 755–758.

- (9) Umakoshi, T.; Udaka, H.; Uchihashi, T.; Ando, T.; Suzuki, M.; Fukuda, T. Quantum-Dot Antibody Conjugation Visualized at the Single-Molecule Scale with High-Speed Atomic Force Microscopy. *Colloids Surf., B* **2018**, *167*, 267–274.

- (10) Shinohara, K. L.; Kodera, N.; Ando, T. Single-Molecule Imaging of a Micro-Brownian Motion of a Chiral Helical  $\pi$ -Conjugated Polymer as a Molecular Spring Driven by Thermal Fluctuations. *Chem. Lett.* **2009**, *38* (7), 690–691.

- (11) Fukui, T.; Uchihashi, T.; Sasaki, N.; Watanabe, H.; Takeuchi, M.; Sugiyasu, K. Direct Observation and Manipulation of Supramolecular Polymerization by High-Speed Atomic Force Microscopy. *Angew. Chem., Int. Ed.* **2018**, *57* (47), 15465–15470.

- (12) Sasaki, N.; Kikkawa, J.; Ishii, Y.; Uchihashi, T.; Imamura, H.; Takeuchi, M.; Sugiyasu, K. Multistep, Site-Selective Noncovalent Synthesis of Two-Dimensional Block Supramolecular Polymers. *Nat. Chem.* **2023**, *15* (7), 922–929.

- (13) Kimura, S.; Adachi, K.; Ishii, Y.; Komiyama, T.; Saito, T.; Nakayama, N.; Yokoya, M.; Takaya, H.; Yagai, S.; Kawai, S.; Uchihashi, T.; Yamanaka, M. Molecular-Level Insights into the Supramolecular Gelation Mechanism of Urea Derivative. *Nat. Commun.* **2025**, *16*, No. 3758.

- (14) Tamaki, K.; Datta, S.; Hanayama, H.; Ganser, C.; Uchihashi, T.; Yagai, S. Photoresponsive Supramolecular Polymers Capable of Intrachain Folding and Interchain Aggregation. *J. Am. Chem. Soc.* **2024**, *146* (32), 22166–22171.

- (15) Maity, S.; Oettel, J.; Santiago, G. M.; Frederix, P. W. J. M.; Kroon, P.; Markovitch, O.; Stuart, M. C. A.; Marrink, S. J.; Otto, S.; Roos, W. H. Caught in the Act: Mechanistic Insight into Supramolecular Polymerization-Driven Self-Replication from Real-Time Visualization. *J. Am. Chem. Soc.* **2020**, *142* (32), 13709–13717.

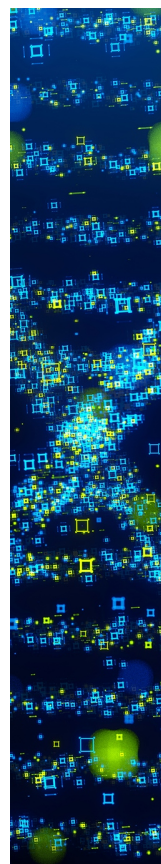
- (16) van Ewijk, C.; Xu, F.; Maity, S.; Sheng, J.; Stuart, M. C. A.; Feringa, B. L.; Roos, W. H. Light-Triggered Disassembly of Molecular Motor-Based Supramolecular Polymers Revealed by High-Speed AFM. *Angew. Chem., Int. Ed.* **2024**, *63* (14), No. e202319387.

- (17) Nishizawa, Y.; Matsui, S.; Urayama, K.; Kureha, T.; Shibayama, M.; Uchihashi, T.; Suzuki, D. Non-Thermoresponsive Decanano-sized Domains in Thermoresponsive Hydrogel Microspheres Revealed by Temperature-Controlled High-Speed Atomic Force Microscopy. *Angew. Chem., Int. Ed.* **2019**, *58* (26), 8809–8813.

- (18) Nishizawa, Y.; Minato, H.; Inui, T.; Uchihashi, T.; Suzuki, D. Nanostructures, Thermoresponsiveness, and Assembly Mechanism of Hydrogel Microspheres during Aqueous Free-Radical Precipitation Polymerization. *Langmuir* **2021**, *37* (1), 151–159.

- (19) Nishizawa, Y.; Yokoi, H.; Uchihashi, T.; Suzuki, D. Single Microgel Degradation Governed by Heterogeneous Nanostructures. *Soft Matter* **2023**, *19* (27), 5068–5075.

- (20) Fukuda, S.; Uchihashi, T.; Iino, R.; Okazaki, Y.; Yoshida, M.; Igarashi, K.; Ando, T. High-Speed Atomic Force Microscope Combined with Single-Molecule Fluorescence Microscope. *Rev. Sci. Instrum.* **2013**, *84* (7), No. 073706.
- (21) Suzuki, Y.; Sakai, N.; Yoshida, A.; Uekusa, Y.; Yagi, A.; Imaoka, Y.; Ito, S.; Karaki, K.; Takeyasu, K. High-Speed Atomic Force Microscopy Combined with Inverted Optical Microscopy for Studying Cellular Events. *Sci. Rep.* **2013**, *3*, No. 2131.
- (22) Umakoshi, T.; Fukuda, S.; Iino, R.; Uchihashi, T.; Ando, T. High-Speed Near-Field Fluorescence Microscopy Combined with High-Speed Atomic Force Microscopy for Biological Studies. *Biochim. Biophys. Acta, Gen. Subj.* **2020**, *1864* (2), No. 129325.
- (23) Yang, K.; Chan, F. Y.; Watanabe, H.; Yoshioka, S.; Inouye, Y.; Uchihashi, T.; Ishitobi, H.; Verma, P.; Umakoshi, T. In Situ Real-Time Observation of Photoinduced Nanoscale Azo-Polymer Motions Using High-Speed Atomic Force Microscopy Combined with an Inverted Optical Microscope. *Nano Lett.* **2024**, *24* (9), 2805–2811.
- (24) Chan, F. Y.; Kurosaki, R.; Ganser, C.; Takeda, T.; Uchihashi, T. Tip-Scan High-Speed Atomic Force Microscopy with a Uniaxial Substrate Stretching Device for Studying Dynamics of Biomolecules under Mechanical Stress. *Rev. Sci. Instrum.* **2022**, *93* (11), No. 113703.
- (25) Ganser, C.; Nishiguchi, S.; Chan, F. Y.; Uchihashi, T. A Look beyond Topography: Transient Phenomena of *Escherichia coli* Cell Division Captured with High-Speed in-Line Force Mapping. *Sci. Adv.* **2025**, *11* (5), No. eads3010.
- (26) Brunsveld, L.; Folmer, B. J. B.; Meijer, E. W.; Sijbesma, R. P. Supramolecular Polymers. *Chem. Rev.* **2001**, *101* (12), 4071–4098.
- (27) De Greef, T. F. A.; Smulders, M. M. J.; Wolfs, M.; Schenning, A. P. H. J.; Sijbesma, R. P.; Meijer, E. W. Supramolecular Polymerization. *Chem. Rev.* **2009**, *109* (11), 5687–5754.
- (28) Aida, T.; Meijer, E. W.; Stupp, S. I. Functional Supramolecular Polymers. *Science* **2012**, *335* (6070), 813–817.
- (29) Lehn, J. M. Supramolecular Polymer Chemistry-Scope and Perspective. *Polym. Int.* **2002**, *51* (10), 825–839.
- (30) Datta, S.; Itabashi, H.; Saito, T.; Yagai, S. Secondary Nucleation as a Strategy towards Hierarchically Organized Mesoscale Topologies in Supramolecular Polymerization. *Nat. Chem.* **2025**, *17*, 477–492.
- (31) Saito, T.; Inoue, D.; Kitamoto, Y.; Hanayama, H.; Fujita, T.; Watanabe, Y.; Suda, M.; Hirose, T.; Kajitani, T.; Yagai, S. Inversion of Supramolecular Chirality by Photo-Enhanced Secondary Nucleation. *Nat. Nanotechnol.* **2025**, *20*, 825–834.
- (32) Yamauchi, M.; Ohba, T.; Karatsu, T.; Yagai, S. Photoreactive Helical Nanoaggregates Exhibiting Morphology Transition on Thermal Reconstruction. *Nat. Commun.* **2015**, *6*, No. 8936.
- (33) Sagara, Y.; Traeger, H.; Li, J.; Okado, Y.; Schrettl, S.; Tamaoki, N.; Weder, C. Mechanically Responsive Luminescent Polymers Based on Supramolecular Cyclophane Mechanophores. *J. Am. Chem. Soc.* **2021**, *143* (14), 5519–5525.
- (34) Thazhathethil, S.; Muramatsu, T.; Tamaoki, N.; Weder, C.; Sagara, Y. Excited State Charge-Transfer Complexes Enable Fluorescence Color Changes in a Supramolecular Cyclophane Mechanophore. *Angew. Chem., Int. Ed.* **2022**, *61* (42), No. e202209225.
- (35) Yamauchi, M.; Adhikari, B.; Prabhu, D. D.; Lin, X.; Karatsu, T.; Ohba, T.; Shimizu, N.; Takagi, H.; Haruki, R.; Adachi, S.; Kajitani, T.; Fukushima, T.; Yagai, S. Supramolecular Polymerization of Supermacrocycles: Effect of Molecular Conformations on Kinetics and Morphology. *Chem. - Eur. J.* **2017**, *23* (22), 5270–5280.
- (36) Yagai, S.; Kubota, S.; Saito, H.; Unoike, K.; Karatsu, T.; Kitamura, A.; Ajayaghosh, A.; Kanetsato, M.; Kikkawa, Y. Reversible Transformation between Rings and Coils in a Dynamic Hydrogen-Bonded Self-Assembly. *J. Am. Chem. Soc.* **2009**, *131* (15), 5408–5410.
- (37) Prabhu, D. D.; Aratsu, K.; Kitamoto, Y.; Ouchi, H.; Ohba, T.; Hollamby, M. J.; Shimizu, N.; Takagi, H.; Haruki, R.; Adachi, S.; Yagai, S. Self-Folding of Supramolecular Polymers into Bioinspired Topology. *Sci. Adv.* **2018**, *4* (9), No. eaat8466.
- (38) Datta, S.; Kato, Y.; Higashiharaguchi, S.; Aratsu, K.; Isobe, A.; Saito, T.; Prabhu, D. D.; Kitamoto, Y.; Hollamby, M. J.; Smith, A. J.; Dagleish, R.; Mahmoudi, N.; Pesce, L.; Perego, C.; Pavan, G. M.; Yagai, S. Self-Assembled Poly-Catenanes from Supramolecular Toroidal Building Blocks. *Nature* **2020**, *583*, 400–405.
- (39) Mabesoone, M. F. J.; Palmans, A. R. A.; Meijer, E. W. Solute–Solvent Interactions in Modern Physical Organic Chemistry: Supramolecular Polymers as a Muse. *J. Am. Chem. Soc.* **2020**, *142* (47), 19781–19798.
- (40) van der Tol, J. J. B.; Vantomme, G.; Meijer, E. W. Solvent-Induced Pathway Complexity of Supramolecular Polymerization Unveiled Using the Hansen Solubility Parameters. *J. Am. Chem. Soc.* **2023**, *145* (32), 17987–17994.
- (41) Isobe, A.; Prabhu, D. D.; Datta, S.; Aizawa, T.; Yagai, S. Effect of an Aromatic Solvent on Hydrogen-Bond-Directed Supramolecular Polymerization Leading to Distinct Topologies. *Chem. - Eur. J.* **2020**, *26* (41), 8997–9004.
- (42) Liu, Q.; Zhang, T.; Ikemoto, Y.; Shinozaki, Y.; Watanabe, G.; Hori, Y.; Shigeta, Y.; Midorikawa, T.; Harano, K.; Sagara, Y. Grinding-Induced Water Solubility Exhibited by Mechanochromic Luminescent Supramolecular Fibers. *Small* **2024**, *20* (33), No. 2400063.
- (43) Ryu, J.-H.; Hong, D.-J.; Lee, M. Aqueous Self-Assembly of Aromatic Rod Building Blocks. *Chem. Commun.* **2008**, No. 9, 1043–1054.
- (44) Lee, J. E.; Lee, N.; Kim, T.; Kim, J.; Hyeon, T. Multifunctional Mesoporous Silica Nanocomposite Nanoparticles for Theranostic Applications. *Acc. Chem. Res.* **2011**, *44* (10), 893–902.
- (45) Görl, D.; Zhang, X.; Würthner, F. Molecular Assemblies of Perylene Bisimide Dyes in Water. *Angew. Chem., Int. Ed.* **2012**, *51* (26), 6328–6348.
- (46) Zhang, X.; Rehm, S.; Safont-Sempere, M. M.; Würthner, F. Vesicular Perylene Dye Nanocapsules as Supramolecular Fluorescent pH Sensor Systems. *Nat. Chem.* **2009**, *1*, 623–629.
- (47) Sagara, Y.; Komatsu, T.; Ueno, T.; Hanaoka, K.; Kato, T.; Nagano, T. Covalent Attachment of Mechanoresponsive Luminescent Micelles to Glasses and Polymers in Aqueous Conditions. *J. Am. Chem. Soc.* **2014**, *136* (11), 4273–4280.



CAS BIOFINDER DISCOVERY PLATFORM™

## STOP DIGGING THROUGH DATA —START MAKING DISCOVERIES

CAS BioFinder helps you find the  
right biological insights in seconds

Start your search

